Interaction of DNA Base Pairs with Various Metal Cations (Mg²⁺, Ca²⁺, Sr²⁺, Ba²⁺, Cu⁺, Ag⁺, Au⁺, Zn²⁺, Cd²⁺, and Hg²⁺): Nonempirical ab Initio Calculations on Structures, Energies, and Nonadditivity of the Interaction

Jaroslav V. Burda,*,† Jiří Šponer,†,‡ Jerzy Leszczynski,§ and Pavel Hobza†

J. Heyrovský Institute of Physical Chemistry, Academy of Sciences of the Czech Republic, Dolejškova 3, 182 23 Prague 8, Czech Republic, Institute of Biophysics, Academy of Sciences of the Czech Republic, Královopolská 135, 612 65 Brno, Czech Republic, and Department of Chemistry, Jackson State University, 1325 J. R. Lynch Street, Jackson, Mississippi 39217-0510
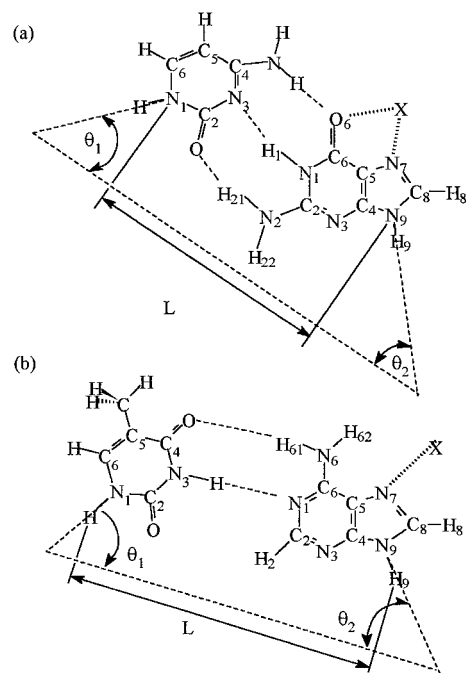
Interaction of Watson−Crick adenine−thymine (AT) and guanine−cytosine (GC) base pairs with various metal (M) cations (Mg²⁺, ..., Hg²⁺) were studied by nonempirical ab initio methods with inclusion of correlation energy. Cations were allowed to interact with the N7 nitrogen of adenine and the N7 and O6 atoms of guanine. All of the cations were described by Christiansen's average relativistic effective potentials using the DZ+P basis set, while the 6-31G** basis set was used for the elements of base pairs. Disruption of the adenine−thymine as well as guanine−cytosine pairs in the presence of all studied cations is energetically more demanding than that for isolated base pairs; the addition stabilization of the base pair is about 100% for complexes with dication. The interaction is highly nonadditive. The three-body term is for the MGC complex considerably larger than that for MAT; the intercomplex charge transfer is also much larger for the former complex.

Introduction

Metal ions interact with many groups in different sites of nucleic acids.[1−6] It is well-known that they not only influence the canonical DNA structures but also are essential in the formation of noncanonical forms of DNA, such as triplexes, quadruplexes, bulges, junctions, etc.[5−7] For example, stabilization of the guanine-quarters by cations originates from cations placed in the center of quarters or shared by two consecutive quarters. The cation is thus coordinated to four or eight guanine carbonyl oxygen atoms.[7] Guanine quarters are mostly stabilized by monovalent cations, perhaps because cumulation of divalent metal ions would lead to too large mutual electrostatic ion−ion repulsion. In general, however, monovalent cations interact primarily with the phosphate groups of the backbone.[2,5,6] Bivalent metal ions can interact with both phosphate and nucleobase, and (mainly transition) metal ions possess significant affinities to nucleobases.[4,6]

In double- or triple-helical structures, the preferred sites for nucleobase−ion interaction are the N7 and O6 positions of guanine (most often a simultaneous binding to both sites) and the N7 position of adenine.[1,6] The metal cations can either interact with the nucleobase directly or through mediation by a water molecule. The cations are always solvated by water molecules, and simultaneous coordination to base and phosphate group is also observed.[5] Cations may interact with other sites on nucleobases (N3 of cytosine, N1 of adenine) that are not accessible under the Watson−Crick base pairing.[4,5] The following order of stability[4] is valid for the transition metal ion binding sites at neutral pH: N7/O6(G) > N3(C) > N7(A) > N1(A) > N3(A,G). The strength of interaction is determined by the interaction of the ion with the molecular electric field of

Figure 1. Structures of the complexes of metal cations with Watson−Crick (a) guanine−cytosine and (b) adenine−thymine pairs. Definition of structural parameters θ₁, θ₂, and L are included.

the nucleobase.[8] Guanine possesses a large dipole moment, and its orientation (cf., e.g.,[9] Figure 1) supports the N7/O6 coordination. Very similar metal ion binding properties are expected for inosine, which has the same dipole moment orientation. The inosine dipole moment is, however, about 20% smaller than that of guanine,[9] so metal ion binding is reduced. On the other hand, the smaller dipole moment of adenine and its orientation[8,9] are responsible for a much weaker metal ion coordination to adenine. The interaction is further reduced in the case of 2-aminoadenine, because this nucleobase has a very low dipole moment of about 1D.[9]

* To whom correspondence should be addressed.
† J. Heyrovský Institute of Physical Chemistry, Academy of Sciences of the Czech Republic.
‡ Institute of Biophysics, Academy of Sciences of the Czech Republic.
§ Jackson State University.
⊗ Abstract published in *Advance ACS Abstracts,* October 15, 1997.

Interaction of DNA Base Pairs with Metal Cations

J. Phys. Chem. B, Vol. 101, No. 46, 1997 **9671**

Direct interaction of metal ions with DNA bases may significantly influence the interactions of nucleic acid bases. For example, Egli and Gessner proposed that polarization of guanine, associated with the metal cation coordination, may stabilize the sugar-base stacking pattern in Z-DNA crystal structures.[10] This hypothesis, however, seems to be ruled out by recent quantum-chemical calculations.[11] Potaman and Soyfer proposed that the metal ion coordination to the N7 position of purines, with its concomitant polarization effects on the bases, influences stabilization of G.GC and A.AT triads in triplexes.[5] This hypothesis was based on, among other data, an ab initio study by Anwander et al.,[12] which predicted enhancement of Watson–Crick base pairing due to the metal ion coordination. One of the main tasks of the present study is to further investigate this possibility. Several recent ab initio studies addressed the binding energetics of divalent alkaline-earth and transition-metal cations to small ligands[13,14] and DNA bases.[8,15] The coordination of transition metal cations is, aside from electrostatic interactions, associated with a covalent-type d-orbital–lone pair bonding interaction, and this (additional) contribution may be responsible for the different affinity of IIa and IIb elements with respect to bases and the phosphodiester backbone in DNA.[16]

Explicit inclusion of metal ions in molecular modeling is frequently used for proper neutralization of the phosphate group charges. To our knowledge, much less attention has been paid to the modeling of the interactions of ions with nucleobases. One of the reasons is the limited ability of the available force fields to deal with such interactions. The current force fields treat metal ions as point charges, and therefore a different nature of interactions of, for example, alkaline earth ions vs transition metal ions could not be described. Furthermore, the set of metal ions available for current force fields is limited. (For example, AMBER 4.1, using the Cornell et al.[17] force field, is parametrized only for Li^+, K^+, Rb^+, and Cs^+ cations.) In addition, the available force fields for DNA modeling are pair additive. Thus, by definition they do not cover any polarization effects or other many-body interactions that might be, in the case of ionic interactions, quite essential. This is also a concern when dealing with DNA structures consisting of protonated base pairs, such as i-DNA and CH^+GC trimers. Nonpolarizable potentials significantly underestimate the base–base attraction in protonated complexes of nucleobases (cf. ref 18), and the importance of developing polarization potentials is now widely accepted.[19–24] However, even the polarizable potentials will not cover another type of interaction: delocalization caused by charge transfer and leading to a covalent-like bonding. Our preceding ab initio study revealed a non-negligible charge transfer in metal ion–base complexes.[8] All of these facts underline the importance of high-level ab initio studies on interactions of metal ions with bases and base pairs.

The use of quantum-chemical methods to study the interactions of metal ions with DNA bases and base pairs was until very recently strongly limited by the availability of sufficiently powerful computer hardware and software. Semiempirical methods do not provide a reliable description even for base–base interactions.[25–27] We investigated interaction of AT pair with various cations in 1985.[28] HF/STO-3G calculations showed that approach of a cation to the thymine O4 leads to destabilization of the pair, while approach of a cation to other available sites (O2 of thymine; N1 and N3 of adenine) results in its stabilization. Recently, Anwander et al.[12] pointed out the possibility of a significant enhancement of base pairing due to metal cation coordination. However, most of the older studies suffer from serious approximations imposed by the computer

resources and programs available. These approximations include the use of minimal basis sets of AO, as well as the disregard of electron correlation effects, molecular relaxation of base pairs upon ion binding, and the basis set superposition error, among other things. Also, the spectrum of metal ions investigated was very narrow. Recent advances in computational quantum chemistry allow for qualitative improvement of such calculations. Previously,[8] we have investigated the interaction of isolated nucleobases with metal ions. The calculations were made with polarized basis sets, electron-correlation effects, and molecular relaxation were included, and the interaction energies were corrected for the basis set superposition error. In addition, the use of effective core pseudopotentials instead of the all-electron approach allowed us to consider a wide range of metal ions. The main aim of the present paper is to characterize complexes of monovalent and divalent metal ions with GC and AT Watson–Crick base pairs. Special attention is given to the origin and magnitude of the nonadditivity of interactions. Our study is consistent with a set of high-level ab initio studies reported on neutral and protonated H-bonded and stacked DNA base pairs.[9,11,18,27–35] The inclusion of hydration, analysis of other base pairs and trimers, inclusion of further metal ions, and an extensive comparison of the ab initio data with available empirical potentials will be presented soon.

Computational Details

Interactions of Watson–Crick (WC) DNA base pairs with alkaline earth metals (Mg^{2+}, Ca^{2+}, Sr^{2+}, Ba^{2+}), coinage metals (Cu^+, Ag^+, Au^+), and zinc group metals (Zn^{2+}, Cd^{2+}, Hg^{2+}) were studied. As in ref 8, cations were described by Christiansen's average relativistic effective potentials (AREP); the original DZ basis sets[36] were augmented by polarization functions taken from the pseudopotentials of Stuttgart's group.[37] Standard 6-31G** basis sets[38] were used for the description of H, C, N, and O atoms of DNA bases. Cations were allowed to interact with nitrogen N7 of adenine in the AT WC pair and with nitrogen N7 and oxygen O6 of guanine in the GC WC pair; structures and numbering of atoms are shown in the Figure 1. The individual positions chosen are known to be active sites in the DNA major groove.[39] The Sr^{2+} cation was considered only in the case of the AT pair; properties of the $Sr^{2+}GC$ complex could be interpolated from properties of $Ca^{2+}GC$, Ba^{2+}-GC, and $Sr^{2+}AT$ complexes.

Geometries of the complexes studied were fully optimized at the HF level with constraint to the planar C_s point group of symmetry. Single-point calculations of the correlation energy were done at the MP2 level for the HF-optimized geometries. All electrons were included in the correlation treatment; i.e., no electrons were kept in "frozen core". Basis set extension effects at the HF and MP2 levels were eliminated using the function counterpoise procedure of Boys–Bernardi;[40] all atomic orbitals of the "ghost" (g) molecule(s) were considered.

Reliability of pseudopotentials was discussed in ref 8. The ionic complexes, as the presently studied ones, are stabilized mainly by Coulombic contributions, covered already at the HF level. Since all of the stabilization energies were evaluated at the MP2 level, we believe that passing to the higher correlated levels does not affect the stabilization energy significantly, as indicated by small differences between HF and MP2 levels.

All structures investigated in the present paper were assumed to be planar. It should be noted that this arrangement does not correspond to a minimum structure for complexes of metal cations with adenine and AT pair. Here, the cation would induce a rotation and pyramidalization of the amino group with

a subsequent coordination of the cation to the N6 nitrogen atom, while keeping the interaction of cation with N7. The energy difference between planar and nonplanar arrangements of adenine$\cdots$Mg^{2+} complex is about 45 kcal/mol at the HF/6-31G** level (because of additional Mg$^{2+}\cdots$N6 interaction), and further energy improvement can be obtained by deprotonation of the amino group with a formation of H1 adenine rare tautomer. The coordination of a cation to N6 destroys the Watson−Crick base pairing (not shown), therefore, we could not study the M$\cdots$AT WC complexes without using the C_s symmetry. In addition, in DNA, the N6 atom should be protected by the solvation shell around the cation. Nevertheless, the interaction between cation and N6 nitrogen atom is currently intensly investigated in our laboratory, including the influence of the water shell around the cation.

Studied complexes could be divided into three subsytems: the two bases (B$_1$, B$_2$) and a metal cation (M). Total interaction energy ($\Delta E'$) is defined as

$$\Delta E' = E(B_1, B_2, M) - [E(B_1) + E(B_2) + E(M)] \quad (1)$$

where $E(B_1, B_2, M)$ means total energy of the whole complex, and $E(B_1)$, $E(B_2)$, and $E(M)$ are total energies of the individual subsystems. Taking the basis set extension effects into account, the total interaction energy (ΔE) is determined as follows:

$$\Delta E = E(B_1, B_2, M) - [E(B_1, gB_2, gM) + E(gB_1, B_2, gM) + \\ E(gB_1, gB_2, M)] \quad (2)$$

Here e.g., $E(B_1, gB_2, gM)$ means total energy of base B$_1$ with basis functions on ghost systems B$_2$ and M. Total interaction energy ΔE could be also defined in terms of pair interaction energies (pairwise energies) and the three-body contribution [$E(3)$]:

$$\Delta E = E(B_1 - B_2) + E(B_1 - M) + E(B_2 - M) + E(3) \quad (3)$$

Each pair interaction energy should be calculated with consideration of basis set extension effects; e.g. for $E(B_1 - B_2)$:

$$E(B_1 - B_2) = E(B_1, B_2, gM) - [E(B_1, gB_2, gM) + \\ E(gB_1, B_2, gM)] \quad (4)$$

Besides these pairwise energies, direct interaction of one subsystem of the complex (metal or pyrimidine) with the remaining ones was also evaluated; e.g., for interaction of thymine with (metal + adenine) subsystem,

$$E(MA - T) = E(A, T, M) - [E(A, gT, M) + E(gA, T, gM)] \quad (5)$$

Results and Discussion

Geometry Parameters. Tables 1−3 show optimized geometry parameters of the complexes studied. The three-body system considered could be described as a composition of a strongly bonded metal cation−purine base complex and weakly bonded metal cation−pyrimidine base and base−base complexes. The latter two pairs represent only a small perturbation of the first one, and their mutual influence is basically very small. Bond lengths and angles between the purine base and ion, optimized in the three-body complex, differ only slightly from these characteristics found in ref 8 for isolated base$\cdots$M pairs (cf. Table 1 of ref 8). The largest bond-length deviation was found for the Ba^{2+}GC complex. The Ba^{2+}−N7 distance in the Ba^{2+}GC complex is 0.08 Å shorter than that found[8] for the Ba^{2+}G complex, with all other bond lengths deviating less. The largest angle deviation was found for the Sr^{2+}AT complex,

TABLE 1: Optimized Base$\cdots$Metal Cation M^{n+} Geometries, Distances (M−N7, M−O6, Å) and Angles (M−N7−C5, deg)

M[a]	guanine[a]		adenine[a]	
	M−N7	M−O6	M−N7	M−N7−C5
Cu$^+$	2.05	2.16	1.98	131.2
Ag$^+$	2.40	2.44	2.28	132.7
Au$^+$	2.28	2.62	2.17	131.0
Zn^{2+}	1.95	1.90	1.87	128.1
Cd^{2+}	2.21	2.17	2.11	128.5
Hg^{2+}	2.23	2.21	2.10	128.8
Mg^{2+}	2.04	1.94	1.96	127.2
Ca^{2+}	2.42	2.30	2.38	129.0
Sr^{2+}			2.55	130.3
Ba^{2+}	2.74	2.53	2.65	131.7

[a] Cf. Figure 1.

TABLE 2: H-Bond Distances (Å) in the Guanine−Cytosine Base Pair in the Three-Body Complex Studied[a]

M	O$_2\cdots$H(N$_2$)	N$_3\cdots$H(N$_1$)	(N$_4$)H$\cdots$O$_6$	θ_1	θ_2	L
Cu$^+$	1.81	2.03	2.34	51.3	58.3	10.12
Ag$^+$	1.87	2.00	2.13	52.4	58.3	10.11
Au$^+$	1.87	1.99	2.13	52.0	58.2	10.12
Zn^{2+}	1.71	1.97	2.47	50.4	62.0	10.02
Cd^{2+}	1.71	2.01	2.46	52.1	62.1	10.02
Hg^{2+}	1.71	2.00	2.46	52.0	62.3	10.01
Mg^{2+}	1.72	1.99	2.47	51.2	61.9	10.03
Ca^{2+}	1.75	2.04	2.43	53.5	61.6	10.04
Ba^{2+}	1.76	2.06	2.45	54.0	61.7	10.05
isol pair	2.02(3.02)	2.03(3.04)	1.91(2.92)	53.0	55.8	10.20
isol pair[b]	(3.03)	(2.90)	(2.93)	51	51	10.35
isol pair[c]	(2.93)	(2.96)	(2.93)	54	52	10.80

[a] Values in parentheses correspond to distances between O$\cdots$N and N$\cdots$N. Parameters θ_1, θ_2, and L are defined in Figure 1. [b] Calculations from ref 12. [c] Experimental values from X-ray diffraction of fibers in ref 39.

TABLE 3: H-Bond Distances (Å) in the Adenine−Thymine Base Pair in the Three-Body Complex Studied[a]

M	O$_4\cdots$H(N$_6$)	(N$_3$)H$\cdots$N1	θ_1	θ_2	L
Cu$^+$	1.93	2.05	55.0	53.4	10.24
Ag$^+$	1.94	2.04	54.9	53.5	10.23
Au$^+$	1.94	2.05	55.1	53.4	10.24
Zn^{2+}	1.75	2.16	54.1	50.1	10.46
Cd^{2+}	1.76	2.15	53.5	51.0	10.40
Hg^{2+}	1.76	2.15	54.1	50.2	10.45
Mg^{2+}	1.75	2.15	53.4	50.1	10.46
Ca^{2+}	1.79	2.12	53.5	51.0	10.40
Sr^{2+}	1.81	2.11	53.5	51.2	10.38
Ba^{2+}	1.81	2.11	53.5	51.2	10.39
isol pair	2.10(3.09)	1.98(2.99)	54.6	55.4	10.13
isol pair[b]	(3.03)	(2.90)	51	51	10.35
isol pair[c]	(2.80)	(3.00)	51	50	11.10

[a] Values in parentheses correspond to distances between O$\cdots$N and N$\cdots$N. Observables θ_1, θ_2, and L are defined in Figure 1. [b] Calculations from ref 12. [c] Experimental values from X-ray diffraction of fibers in ref 39.

where the Sr^{2+}−N7−C5 angle is about 6° smaller than the corresponding angle in the Sr^{2+}A complex; other angles differ by less than 5° from their respective angles in the M−purine systems.

Let us compare our geometries with results reported by Anwander et al.[12] for complexes with Ca^{2+}, Mg^{2+}, and Zn^{2+}. First, the use of a minimal basis set leads to distances that are too short between the purine base and the metal cation, especially for the Zn^{2+} complexes (this work predicts 1.95 Å for the Zn^{2+}GC complex, while Anwander et al.[12] reported 1.72 Å). Also, M−N7−C5 bond angles differ in the MAT complexes; our values are larger by about 10° for the Mg^{2+}AT

Interaction of DNA Base Pairs with Metal Cations

J. Phys. Chem. B, Vol. 101, No. 46, 1997 **9673**

TABLE 4: Mulliken Partial Charges (e) on Selected Atoms of the MGC and MAT Complexes

M^b	MGC[a]					MAT[a]			
	M	N7	O6	H21	H1	M	N7	N1	H61
Cu^+	0.92	−0.81	−0.82	0.44	0.42	0.92	−0.95	−0.73	0.42
Ag^+	0.76	−0.69	−0.76	0.44	0.42	0.81	−0.79	−0.74	0.41
Au^+	0.73	−0.72	−0.73	0.44	0.42	0.73	−0.81	−0.73	0.41
Zn^{2+}	1.73	−1.05	−0.97	0.46	0.46	1.73	−1.21	−0.69	0.46
Cd^{2+}	1.45	−0.82	−0.82	0.45	0.45	1.54	−0.93	−0.69	0.46
Hg^{2+}	1.40	−0.81	−0.79	0.45	0.46	1.43	−0.98	−0.69	0.46
Mg^{2+}	1.77	−1.00	−0.98	0.46	0.45	1.83	−1.18	−0.69	0.46
Ca^{2+}	1.84	−0.90	−0.94	0.44	0.44	1.88	−1.02	−0.70	0.45
Sr^{2+}						1.91	−0.98	−0.71	0.45
Ba^{2+}	1.73	−0.80	−0.88	0.44	0.44	1.81	−0.91	−0.71	0.45
isol pair		−0.52	−0.68	0.39	0.41		−0.56	−0.77	0.38

[a] Cf. Figure 1.

and Ca^{2+}AT complexes, while for the Zn^{2+}AT complexes we predict smaller M−N7−C5 angles, by about 20°. Table 1 shows that the displacement from the average value of this M−N7−C5 angle is not so pronounced for complexes containing zinc-group elements as it is for metals of alkaline earths. In the case of MGC complexes, there are smaller differences in the M−N7−C5 angles between the two studies, because the coordination of the ion to two atoms leads to a less-flexible system. However, let us recall that, in contrast to our study, data by Anwander et al. are not based on gradient optimization. They used base-pair geometries from the experimental structures (without ions), and the positions of the metal ions and their distances to the bases were taken from optimized ion−base dimers where the geometry of the base was held rigid.[42]

The pyrimidine base B_2 has only a negligible influence on the metal−purine system. However, the metal ion significantly influences the geometry of the base pair. Tables 2 and 3 summarize H-bond lengths in the base pairs under metal ion coordination. The O···H(N2) H-bond lengths in the GC complexes are systematically reduced, in comparison with the isolated pair. This reduction is largest for bivalent ions (0.3 Å). The central H-bond H···N1 in the GC complexes remains practically unchanged, and the third H···O6 H-bond, which is closest to the metal cation, is significantly lengthened in comparison with the isolated GC pair. The lengthening is largest for bivalent ions (0.65 Å in Zn^{2+}GC and Mg^{2+}GC). In the AT pair, the metal cations affect the H-bonds in a different way. The H···N6 H-bond, which is closer to the metal ion coordination site, shows substantial shortening (0.35 Å in complexes with Zn^{2+} and Mg^{2+}), while the other H-bond (H···N1) is lengthened (by 0.18 Å in Zn^{2+}AT complex).

Changes in AT and GC H-bond lengths could be interpreted in several ways. The first interpretation is based on the modified charge density of atoms participating in the H-bond under the influence of metal cations. As mentioned in our previous study,[8] metal cation coordination to the adenine N7 position induces a shift of electron density toward the metal cation. In this way the decrease of negative charge on N1 (−0.77 e in isolated adenine, −0.73 e in M^+AT, and −0.69 e in M^{2+}AT; cf. Table 4) and increase of positive charge on H(N6) (0.38 e in isolated adenine, 0.41 e in M^+AT, 0.45 e in M^{2+}AT) can be observed. Cation binding to guanine in GC pair leads to an increase of negative partial charge on O6 (−0.68, −0.77, and −0.90 e for GC, M^+GC, and M^{2+}GC, respectively), and also of positive charge on H(N1) (0.41, 0.44, 0.45 e) and H(N2) (0.29, 0.42, 0.45 e) atoms. Partial electron charges in Table 4 are based on Mulliken population analysis, but basically the same trends were also observed from NBO analysis (not shown). From the point of increased negative charge on O_6, shortening of the O6···H-

(N_4) H-bond was expected; however, this was not found (see above). This indicates that our explanation of geometry changes in terms of induced charges is not complete. Another important factor is a direct electrostatic repulsion between the metal cation and the closest atom of cytosine, the H(N4) hydrogen. (They are separated by about 4.2 Å.) Also, the anisotropic distribution of the electron charge on O6 (due to the polarization toward the metal ion) partially reduces the strength of the O6···H(N4) H-bond. Shortening of the (N2)H···O2 H-bond is in accord with both the increased positive charge on H(N2) and the geometry induced by the above-mentioned repulsion between M and H(N4).

The geometric rearrangements of the pair structures can be regarded as rotation around the center of the pyrimidine ring toward the metal cation in the case of the AT pair, and away from it in the case of the GC pair. This can be demonstrated by orientational parameters θ_1, θ_2, and L of the base pairs (for definitions, see Figure 1) in Tables 2 and 3. AT-containing pairs, in particular, show smaller θ_2 angles and longer L (55°, 10.1 Å in isolated base pair; 53°, 10.2 Å in monovalent cation complexes; and 50−51°, 10.4 Å in bivalent ones). The same θ_2 parameter exhibits larger angles simultaneously with shorter L values in GC pairs. Tables 2 and 3 also present previous computational[12] as well as experimental[41] data. It should be noted that the geometry changes of base pairing could also be discussed in terms of the orientation of molecular dipole moments of both the purine and pyrimidine with respect to the metal ion (see below).

Energy Characteristics. Main energy characteristics for MAT and MGC complexes are shown in Tables 5 and 6. The tables summarize all three pairwise contributions, three-body term, binding energy between the ion and the base pair, "base pairing" energy between the purine ion complex and pyrimidine, and, finally, total interaction energy of the complex.

Basically the same dependencies of the stabilization energies vs increasing atomic number of metal cation are observed for metal−purine−pyrimidine complexes and previously published metal−purine complexes. (See Figure 2 in ref 8). This means that we can regard the H-bonded pyrimidine base as a weak perturbation of the metal−purine complexes. Stabilization energies of complexes with bivalent ions are larger than those of monovalent ions, and M−GC stabilization energies are larger than those for M−AT complexes. Both of these conclusions reflect the dominant role of the ion−dipole electrostatic contribution to the stabilization energy of the complex, as well as the fact that the dipole moment of the GC WC base pair is larger than that of the AT WC base pair.

Compared with the previous study,[12] very close agreement was obtained for complexes of Ca^{2+} with base pairs (within 5kcal/mol) but larger differences were found in Mg^2-containing systems (~20 kcal Mg^{2+}AT and ~40 kcal Mg^{2+}GC; the values in present work are higher—more stabilizing—for both base pairs). The use of a minimal basis set (MBS) for zinc[12] (all-electron calculations) nearly doubles the stability (ΔE^{HF}(MBS: Zn^{2+}GC) = −448 kcal/mol vs present ΔE^{HF}(AREP:Zn^{2+}GC) = −254 kcal/mol and ΔE^{HF}(MBS:Zn^{2+}AT) = −328 kcal/mol vs ΔE^{HF}(AREP:Zn^{2+}AT) = −158 kcal/mol; all values are BSSE corrected). A similar conclusion about overestimation of the stabilization energies by MBS can also be made when comparing the interaction of an ion with a single nucleobase (adenine or guanine), cf. refs 8 and 12.

The detailed energy analysis of the metal cation−base pair complex must be based on the study of the three-body system. There are two possibilities how to handle the whole system. First, two-body interaction energies and the three-body term

TABLE 5: Interaction Energies of the System Metal Cation−Adenine−Thymine (kcal/mol) Obtained at the HF and MP2 Levels[a]

metal	method	$E(M-A)$	$E(M-T)$	$E(A-T)$[b]	$E(3)$	$E(M-AT)$	$E(MA-T)$	$E(M-A-T)$
Cu^+	HF	−43.61	−4.54	−9.76	−0.13	−48.28	−14.42	−58.04
Cu^+	MP2	−54.45	−4.09	−11.98	−0.03	−58.57	−16.09	−70.54
Ag^+	HF	−31.30	−4.43	−9.79	−0.10	−35.83	−14.32	−45.62
Ag^+	MP2	−36.02	−3.99	−12.00	−0.02	−40.03	−16.02	−52.03
Au^+	HF	−42.29	−4.50	−9.81	−0.06	−46.86	−14.37	−56.66
Au^+	MP2	−55.03	−4.06	−12.02	0.00	−59.09	−16.08	−71.12
Zn^{2+}	HF	−144.34	−11.25	−8.36	−2.4	−157.99	−22.01	−166.35
Zn^{2+}	MP2	−152.89	−[c]	−10.81	−[c]	−165.86	−23.78	−176.67
Cd^{2+}	HF	−109.87	−11.19	−8.47	−2.15	−123.21	−21.81	−131.68
Cd^{2+}	MP2	−116.63	−[c]	−10.91	−[c]	−129.29	−23.56	−140.19
Hg^{2+}	HF	−126.38	−11.01	−8.50	−2.27	−139.66	−21.79	−148.16
Hg^{2+}	MP2	−141.07	−[c]	−10.93	−[c]	−153.81	−23.67	−164.74
Mg^{2+}	HF	−111.12	−11.45	−8.37	−2.10	−124.68	−21.93	−133.05
Mg^{2+}	MP2	−107.93	−[c]	−10.82	−[c]	−120.66	−23.54	−131.47
Ca^{2+}	HF	−63.84	−10.99	−8.67	−1.50	−76.33	−21.16	−85.00
Ca^{2+}	MP2	−61.57	−10.03	−11.08	−1.50	−73.10	−22.62	−84.18
Sr^{2+}	HF	−51.04	−10.65	−8.79	−1.25	−62.94	−20.69	−71.73
Sr^{2+}	MP2	−48.88	−9.72	−11.18	−1.21	−59.81	−22.11	−70.99
Ba^{2+}	HF	−49.05	−10.40	−8.83	−1.36	−60.81	−20.60	−69.65
Ba^{2+}	MP2	−51.43	−9.51	−11.22	−1.36	−62.30	−22.09	−73.52

[a] $E(M-A)$, $E(M-T)$, and $E(A-T)$ are the respective pairwise contributions, $E(3)$ is the three-body term, $E(M-AT)$ is the binding energy between cation and the base pair, $E(MA-T)$ is the base pair strength upon inclusion of the cation interactions, and $E(M-A-T)$ is the total interaction energy of the complex. [b] HF and MP2 interaction energies for isolated pair adenine···thymine are −10.3 and −12.3 kcal/mol, respectively (6-31G** basis set; BSSE considered). [c] MP2 interaction energies could not be evaluated because of the orbital mixing—see the last paragraph in the part Energy Characteristics.

TABLE 6: Interaction Energies of the System Metal Cation−Guanine−Cytosine (kcal/mol) Obtained at HF and MP2 Levels[a]

metal	method	$E(M-G)$	$E(M-C)$	$E(G-C)$[b]	$E(3)$	$E(M-GC)$	$E(MG-C)$	$E(M-G-C)$
Cu^+	HF	−73.95	0.13	−26.63	−5.24	−79.06	−31.74	−105.70
Cu^+	MP2	−79.99	0.16	−27.19	−6.27	−86.11	−33.31	−113.29
Ag^+	HF	−61.65	0.65	−26.44	−4.58	−65.58	−30.37	−92.02
Ag^+	MP2	−64.22	0.64	−27.06	−5.43	−69.00	−31.85	−96.06
Au^+	HF	−65.88	0.32	−26.36	−5.17	−70.73	−31.21	−97.09
Au^+	MP2	−75.92	0.34	−27.05	−6.18	−81.76	−32.89	−108.81
Zn^{2+}	HF	−234.94	−4.59	−25.98	−15.04	−254.57	−45.62	−280.55
Zn^{2+}	MP2	−237.24	−[c]	−26.08	−[c]	−259.36	−48.19	−285.43
Cd^{2+}	HF	−190.46	−4.32	−25.74	−12.05	−206.84	−42.11	−232.57
Cd^{2+}	MP2	−192.60	−[c]	−25.96	−[c]	−211.26	−44.62	−237.22
Hg^{2+}	HF	−196.67	−4.31	−25.68	−12.94	−213.91	−42.92	−239.59
Hg^{2+}	MP2	−207.98	−[c]	−25.90	−[c]	−227.99	−45.91	−253.88
Mg^{2+}	HF	−209.68	−6.32[d]	−25.85	−11.04[d]	−227.04	−43.21	−252.89
Mg^{2+}	MP2	−198.65	−[c]	−25.95	−[c]	−217.83	−45.13	−243.78
Ca^{2+}	HF	−143.49	−2.95	−25.49	−8.82	−155.26	−37.26	−180.75
Ca^{2+}	MP2	−133.87	−2.97	−25.75	−10.06	−146.90	−38.78	−172.65
Ba^{2+}	HF	−120.55	−1.86	−25.28	−8.34	−130.75	−35.49	−156.04
Ba^{2+}	MP2	−118.83	−2.02	−25.58	−9.62	−130.47	−37.21	−156.05

[a] $E(M-G)$, $E(M-C)$, and $E(G-C)$ are the respective pairwise contributions, $E(3)$ is the three-body term, $E(M-GC)$ is the binding energy between cation and the base pair, $E(MG-C)$ is the base pair strength upon inclusion of the cation interactions, and $E(M-G-C)$ is the total interaction energy of the complex. [b] HF and MP2 interaction energies for isolated pair adenine···thymine are −25.5 and −26.3 kcal/mol, respectively (6-31G** basis set; BSSE considered). [c] MP2 interaction energies could not be evaluated because of the orbital mixing—see the last paragraph in the part Energy Characteristics. [d] Connected with $\delta(Mg) = 1.83$ instead of $\delta(Mg) = 2.00$ (cf. the Energy Characteristics discussion).

can be obtained by eqs 2−4 for individual MAT and MGC complexes in pairwise treatment. Second, the direct influence of H-bonded base pairs by metal cation $E(MA-T)$ and $E(MG-C)$ (and, similarly, the influence of the metal−purine part by the pyrimidine base $E(M-AT)$ and $E(M-GC)$) are defined according to the eq 5.

Let us start the discussion of the pairwise terms, with the H-bond interaction. H-bonds in the AT pair within the MAT complexes are systematically weakened in comparison with the isolated optimized AT pair ($\Delta E^{HF} = -10.3$ kcal/mol, $\Delta E^{MP2} = -12.3$ kcal/mol). This weakening, which is the largest for bivalent ions, is due to the change in base−base geometry induced by ions (cf. Tables 2 and 3, and the discussion above). The largest geometry changes with respect to the isolated pair are induced by bivalent ions. A similar weakening of H-bonds was expected to occur in the MGC complexes. However, from

Table 6 we found that ΔE^{HF} of H-bonds in the GC pair within the MGC complexes are a little stronger (with $Ca^{2+}-Ba^{2+}$ exception) than those H-bonds in the isolated GC pair. In the case of complexes with Cu^+-Au^+ monocations even ΔE^{MP2} base pair stabilization energies are greater than the corresponding H-bond energy of the isolated GC pair ($\Delta E^{HF} = -25.5$ kcal/mol, $\Delta E^{MP2} = -26.3$ kcal/mol). It is also clear that, in the case of MGC complex, the geometry of GC base pair is deformed by metal cation coordination. However, the deformation of molecular geometry of guanine is connected with the increase of its HF dipole moment by more than 1D (e.g. from $\mu = 7.1$ D in isolated GC pair to $\mu = 8.0$ D in the Cu^+GC complex and $\mu = 8.9$ D in the $Zn^{2+}GC$ structure). It results in increased dipole−dipole interaction between bases, which successfully compensates for the decreased H-bond interaction caused by deformation of GC pair geometry. Since the

TABLE 7: Charge Transfer among Individual Parts of Three-Body Complexes, Based on Mulliken Population Analysis

metal	δ(metal)	δ(adenine)	δ(thymine)	δ(metal)	δ(guanine)	δ(cytosine)
Cu^+	0.92	0.06	0.02	0.92	0.02	0.07
Ag^+	0.81	0.17	0.02	0.76	0.18	0.07
Au^+	0.73	0.25	0.02	0.73	0.21	0.06
Zn^{2+}	1.73	0.22	0.05	1.73	0.16	0.11
Cd^{2+}	1.54	0.41	0.05	1.45	0.45	0.10
Hg^{2+}	1.43	0.52	0.05	1.40	0.50	0.10
Mg^{2+}	1.83	0.12	0.05	1.77	0.13	0.10
Ca^{2+}	1.88	0.08	0.05	1.84	0.07	0.09
Sr^{2+}	1.91	0.05	0.04			
Ba^{2+}	1.81	0.15	0.04	1.73	0.18	0.09
isol pair		0.01	−0.01		−0.03	0.03

deformed H-bond geometries are not too different from those of the isolated base pairs for monocations of coinage metals, the reduced MP2 dipole moments fully compensate for the deformations of H-bonds. Hence even the MP2 H-bonding is slightly stronger than that for isolated GC pair. Similar increases in dipole moments of adenine were not observed in MAT complexes. This paragraph can be closed by stating that H-bond strength of GC or AT pairs, calculated as a pairwise interaction energy within the optimized MGC or MAT complexes, is influenced only slightly by cations.

The second pairwise term describes the metal cation−purine complex. The ion−adenine stabilization energies within the MAT complex are systematically reduced in comparison with the isolated MA pair. The same is true for ion−guanine stabilization energies within the MGC complex. In the previous paragraph, the increase of the two-body GC stabilization energies in comparison with isolated pair was explained by dipole moment changes. Here the decrease of the metal cation−G stabilization, in comparison with the isolated metal− guanine stabilization, can be explained by the fact that the same geometry deformations (connected with the higher dipole moment) occur already in the metal cation−guanine system; i.e., there is no further change in guanine dipole moment when complexation with cytosine takes place.

The last pairwise terms are the interactions of ions with remote (pyrimidine) bases. They are relatively large (in comparison with H-bond interaction) and always attractive in the case of the AT pair. The decreased values of MP2 interaction energies with respect to the HF values can be explained as follows. The main contribution to the total MP2 interaction energy is the long-range electrostatic term. When passing from the HF to MP2 level, the very weak attractive dispersion terms between ion and remote base are not capable of compensating for the reduction of electrostatic contributions, which is due to the smaller thymine dipole moment predicted from the correlated wave function. The same arguments also hold in the case of the GC pair. However, in this case the dipole moment of cytosine is nearly perpendicular to the connection between the metal ion and the center of mass of cytosine; i.e., the dipole−ion interaction is weak. There is an additional effect that should be considered in this case. The closest atom of the base to the cation is the positively charged H(N4) hydrogen of cytosine (contrary to the negatively charged O4 atom in thymine case), which causes strong repulsion of both parts. Repulsive metal−pyrimidine interactions for monovalent coinage metals and attractive interactions for bivalent metals are due to the different position of cytosine in the MGC complexes: H(N4) of cytosine is closer to the metal in the case of monovalent ions. Dications act more strongly on the pyrimidine base and "push" it to a more advantageous position from the ion−dipole moment point of view, which is connected with larger deformation of H-bonded base pairs. In terms of competing metal− pyrimidine and H-bond interactions, it can be seen in Tables 5

and 6 that the H-bond energies are higher (i.e., more attractive) in both the G−C and A−T pairs for monovalent than for bivalent cations.

The three-body term, which is connected with pairwise energies and total interaction energy through eq 3, gives basic information about nonadditivity to pair interactions. From Tables 5 and 6 it is clear that this term is small for MAT complexes, while it is considerably larger for MGC ones. As expected, the three-body term is always larger for bivalent ions than for monovalent ones.

The main contributions to the three-body nonadditivity represent the induction nonadditivities basically covered at the HF level. Induction energy (and also induction nonadditivities) depends on charge of one system and polarizability of the other system. Therefore, one might expect that the induction non-additivities will be larger for bivalent ions than for monovalent ions, and for GC than for AT pair. However the qualitative difference between the three-body terms for GC and AT pair cannot be explained solely on the basis of polarizability. Thus also charge transfer (CT) effects are important. The larger three-body term for MGC pair is accompanied by larger CT within the complex. Table 7 displays CT evaluated on the basis of the Mulliken populations for different parts of the complex. Despite that, in general, CT is larger from metal to GC base pair than to AT base pair, the total charge on guanine is usually smaller than the corresponding value for adenine. In other words, there is an additional significant CT to cytosine. Table 7 shows that the positive partial electron charge on cytosine is twice as high as the charge on thymine. Thus, the (additional, "CT") metal−thymine electrostatic repulsion is smaller than the metal−cytosine interaction. On the contrary, the higher portion of the cytosine electron density is induced toward the space between all the three parts of the M−G−C complex and can act as an additional "bonding" electron density. For selected systems (Ca^{2+},Zn^{2+},Cu^+−AT/GC) the NBO analysis has been done, and the results were similar to those based on the Mulliken population.

Finally, let us discuss the direct interaction energies E(M− AT) and E(M−GC) for the interaction of metal with base pairs, and E(MA−T) and E(MG−C) terms for the interaction (pairing) of metal cation-purine subsystem with pyrimidine base. The former value corresponds to the sum of pairwise interaction energies E(M−Pu) + E(M−Py) + E(3), showing how the metal−purine interaction will be increased in the presence of the remote H-bonded pyrimidine base. From Tables 5 and 6, it follows that additional stabilization by the pyrimidine base acting on metal−purine subsystem can be up to 19.6 kcal (Zn^{2+}-GC complex). The E(MA−T) and E(MG−C) interactions can be expressed as the sum of E(M−Py) + E(Pu−Py) + E(3). These values indicate how coordination of the metal ion influences the stability of the base pairs. Tables 5 and 6 show that the MA−T and MG−C interactions are considerably stronger than the A−T or G−C ones. This effect is more

pronounced for bivalent ions, and Mg^{2+} amplifies the binding by more than 100% in the case of the $Mg^{2+}AT$ complex and by about 70% in the case of the $Mg^{2+}GC$ complex. In other words, whereas the disruption of the AT pair requires about 10 kcal/mol in isolated system, it requires more than 22 kcal/mol in the $Mg^{2+}AT$ complex. Similarly, disruption of base pairing in isolated GC base pair and the $Mg^{2+}GC$ complex requires about 25 and 43 kcal/mol, respectively. This unambiguously shows how the base pairing changes when a metal cation approaches base pair and interacts with it.

To conclude the energy discussion, we would like to mention one difficulty connected with evaluations of total energies $E(X-gG-C)$ and $E(X-gA-T)$ in the case of BSSE corrections calculations for Mg^{2+}, Zn^{2+}, Cd^{2+}, and Hg^{2+}. The ground-state energies of these systems are not consistent with the model we used: instead of the expected charge distribution of 2+ on metal and zero on cytosine or thymine, a part of the charge density is shifted from the metal cation to the pyrimidine base. This situation corresponds to the dissociation to monovalent or neutral metal and pyrimidine base cation or dication. Similar states were described in ref 43 using semiempirical method. Energies consistent with our model (dissociation to metal 2+ and neutral pyrimidine base) lie above the energies of the latter distribution; it was therefore necessary to start an energy calculation from correct dissociation limits and then gradually bring the metal to the pyrimidine base, which remains centered in optimized geometry together with the Gaussian functions of the ghost purine base. In this way, we were able to obtain the required energies (except of $Mg^{2+}GC$ complex, where even using a very tiny step for the approach of both parts in the 0.65–0.64 Å interval, we cannot prevent at least partial mixing, leading to the charge distribution $\delta(Mg) = 1.83$ e instead of $\delta(Mg) = 2.00$ e, cf. Table 6). However, the HOMO eigenvalues were smaller than LUMO eigenvalues in these cases. Hence, the MP2 energies were not calculated. This fact is connected with the mutual mixing of the LUMO (vacant s-AO of these metal cations, which has relatively low orbital energy; e.g., 4s AO of Zn: $\epsilon = -0.616$ hartree) and some of the higher occupied MOs (e.g., in the $Zn-gG-C$ case, these orbitals originate with cytosine, and the HOMO of the isolated cytosine molecule has $\epsilon = -0.336$). In the mentioned $Zn-gG-C$ system, the strong orbital interaction of the original (unmixed orbitals) system HOMO-2 ($\epsilon = -0.555$) and LUMO ($\epsilon = -0.608$) was found to be what led to their mixing and the creation of a new set of "wrong" MOs where HOMO-2 ($\epsilon = -0.607$) appears with a partial presence of Zn 4s AO. The LUMO energy ($\epsilon = -0.524$) lies now above HOMO level.[44] As a result, the transfer of some portion of electron density from cytosine to the 4s orbital of Zn occurs, which decreases the charge on the Zn^{2+} cation from +2 to +1.34. For example, the energy differences between the two states with proper ($\delta(Zn^{2+}) = \delta(Hg^{2+}) = 2.00$ e) and incorrect ($\delta(Zn^{2+}) = 1.34$ e, $\delta(Hg^{2+}) = 0.96$ e) charge population are $\Delta E(Zn^{2+}GC) = 27.6$ kcal/mol in case of Zn^{2+}-GC and $\Delta E(Hg^{2+}AT) = 57.3$ kcal/mol in case of $Hg^{2+}AT$.

Biological Consequences. Metallic cations bound to the WC base pairs dramatically (directly or indirectly) change many aspects of the base pairing. If metallic cations are located at the positions investigated in the present paper, the rupture of base pairing requires considerably more energy. (If the ion is placed at other places around the base pair, the disrupture of the base pair may result; see our previous paper.[28]) The interactions are characterized by strong nonadditivities that (by definition) cannot be covered by the empirical potentials. This makes the ab initio treatment attractive and important. Our very preliminary data[16] indicate that the three-body term for

complexes of cations with the third strand-forming reverse Hoogsteen GG base pair in G.GC triplexes is even more pronounced than those for the GCWC pair, and significantly contributes to the triplex stabilization. This would mean that the nonadditivity is larger (in absolute value) than is the contribution from the reverse Hoogsteen base pairing itself. Understanding the interaction of metallic ions with DNA base pairs is quite essential in order to rationalize the role of metal cations in nucleic acid structure and interactions. One should also keep in mind that the interaction of metal cations with bases and base pairs cannot be satisfactorily evaluated by the currently available atom–atom pairwise empirical potentials. We are aware that water molecules can significantly modify the picture of metal cation- base pair interactions. Work is in progress in our laboratory to explicitly include the first hydration shell into the calculations.

References and Notes

(1) Eichhorn, G. L. *Adv. Inorg. Chem.* **1981**, *3*, 1.
(2) Sanger, W. Principles of Nucleic Acids Structure; Springer-Verlag: New York, 1984.
(3) Martin, R. B. *Acc. Chem. Res.* **1985**, *18*, 32.
(4) Sigel, H. *Chem. Soc. Rev.* **1993**, *18*, 32.
(5) Potaman, V. N.; Soyfer, V. N. *J. Biomol. Struct. Dyn.* **1994**, *11*, 1035.
(6) Sabat, M.; Lippert, B. In *Metal Ions in Biol. Systems. Vol. 33*; Sigel, A., Sigel H., Eds.; Marcel Dekker, Inc.: New York, 1996; p 143.
(7) Guschlbauer, W.; Chantot, J. F.; Thiele, D. *J. Biomol. Struct. Dyn.* **1990**, *8*, 491.
(8) Burda, J. V.; Šponer, J.; Hobza, P. *J. Phys. Chem.* **1996**, *100*, 7250.
(9) Šponer, J.; Leszczynski, J.; Hobza, P. *J. Phys. Chem.* **1996**, *100*, 1965.
(10) Egli, M.; Gessner, R. V. *Proc. Natl. Acad. Sci. U.S.A.* **1995**, *92*, 180.
(11) Šponer, J.; Gabb, A. H.; Leszczynski, J.; Hobza, P. *Biophys. J.* **1997**, *73*, 76.
(12) Anwander, E. H. S.; Probst, M. M.; Rode, B. M. *Biopolymers* **1990**, *29A*, 757.
(13) Garmer, D. R.; Gresh, N. *J. Am. Chem. Soc.* **1994**, *116*, 3556.
(14) Gresh, N.; Garmer, D. R. *J. Comput. Chem.* **1996**, *17*, 1481.
(15) Del Bene, J. E. *J. Phys. Chem.* **1984**, *88*, 5927.
(16) Šponer, J.; Burda, J. V.; Mejzlik, P.; Leszczynski, J.; Hobza, P. *J. Biomol. Struct. Dyn.* **1997**, *14*, 613.
(17) Cornell, W. D.; Cieplak, P.; Bayly, C. I.; Gould, I. R.; Merz, K. M., Jr.; Feguson, D. M.; Spellmeyer, D. C.; Fox, T.; Caldwell, J. W.; Kollman, P. A. *J. Am. Chem. Soc.* **1995**, *117*, 5179.
(18) Šponer, J.; Leszczynski, J.; Vetterl, V.; Hobza P. *J. Biomol. Struct. Dyn.* **1996**, *13*, 695.
(19) Alkorta, I.; Perez. J. J. *Int. J. Quantum. Chem.* **1996**, *57*, 123.
(20) Bernardo, D. N.; Ding, Y. B.; Krogh-Jespersen, K.; Levy, R. M. *J. Phys. Chem.* **1994**, *98*, 4180.
(21) Caldwell, J. W.; Kollman, P. A. *J. Phys. Chem.* **1995**, *99*, 6208.
(22) Ding, Y.; Bernardo, D. N.; Krogh-Jespersen, K.; Levy, R. M. *J. Phys. Chem.* **1995**, *99*, 11575.
(23) Halgren, T. A. *Curr. Opin. Struct. Biol.* **1995**, *5*, 205.
(24) Sun, Y.; Caldwell, J. W.; Kollman, P. A. *J. Phys. Chem.* **1995**, *99*, 10081.
(25) Hobza, P.; Hubálek, F.; Kabelác, M.; Mejzlík, P.; Šponer, J.; Vondrášek, *J. Chem. Phys. Lett.* **1996**, *257*, 31.
(26) Hobza, P.; Kabelác, M.; Mejzlík, P.; Šponer, J.; Vondrášek, J. *J. Comput. Chem.* **1997**, *18*, 1136.
(27) Šponer, J.; Leszczynski, J.; Hobza, P. *J. Biomol. Struct. Dyn.* **1996**, *14*, 117.
(28) Hobza, P.; Sandorfy, C. *J. Biomol. Struct. Dyn.* **1985**, *6*, 1245.
(29) Gould, I. R.; Kollman, P. A. *J. Am. Chem. Soc.* **1994**, *116*, 2493.
(30) Hobza, P.; Šponer, J.; Polášek, M. *J. Am. Chem. Soc.* **1995**, *117*, 792.

(31) Šponer, J.; Hobza, P. *J. Biomol. Struct. Dyn.* **1994**, *12*, 671.

(32) Florián, J.; Leszczynski, J. *J. Biomol. Struct. Dyn.* **1995**, *12*, 1055.

(33) Florián, J.; Leszczynski, J. *J. Am. Chem. Soc.* **1996**, *118*, 3010.

(34) Šponer, J.; Leszczynski, J.; Hobza, P. *J. Phys. Chem.* **1996**, *100*, 5590.

(35) Šponer, J.; Leszczynski, J.; Hobza; P. *J. Comput. Chem.* **1996**, *17*, 841.

(36) (a) Pacios, L. F.; Christiansen, P. A. *J. Chem. Phys.* **1985**, *82*, 2664. (b) Hurley, M. M.; Pacios, L. F.; Christiansen, P. A.; Roos, R. B.; Ermler, W. C. *J. Chem. Phys.* **1986**, *84*, 6840. (c) LaJohn, L. A.; Christiansen, P. A.; Roos, R. B.; Atashroo, T.; Ermler, W. C. *J. Chem. Phys.* **1987**, *87*, 2812. (d) Roos, R. B.; Powers, J. M.; Atashroo, T.; Ermler, W. C.; LaJohn, L. A.; Christiansen, P. A. *J. Chem. Phys.* **1990**, *93*, 6654.

(37) (a) Kaupp, M.; Schleyer, P. v. R.; Stoll, H.; Preuss, H. *J. Chem. Phys.* **1991**, *94*, 1360. (b) Kaupp, M.; Schleyer, P. v. R.; Stoll, H.; Preuss, H. *J. Chem. Phys.* **1991**, *94*, 1360.

(38) Ditchfield, R.; Hehre, W. J.; Pople, J. A. *J. Chem. Phys.* **1972**, *56*, 2257.

(39) Martin R. B. In *Metal Ions in Biol. Systems. Vol. 32*; Sigel, A., Sigel, H., Eds.; Marcel Dekker, Inc.: New York, 1995; pp 61−88.

(40) Boys, S. F.; Bernardi, F. *Mol. Phys.* **1970**, *19*, 553.

(41) Pauling, L.; Corey, R. *Arch. Biochem. Biophys.* **1956**, *65*, 164.

(42) (a) Sagarik, K.; Rode B. *Inorg. Chem. Acta* **1983**, *76*, L209. (b) Anwander, E.; Probst, M.; Rode, B. *Inorg. Chem. Acta* **1987**, *137*, 203.

(43) Lipinski, J. *J. Mol. Struct. (THEOCHEM)* **1989**, *201*, 87.

(44) Color postscript picture of this textbook mixing is available from the author upon request.